Received 20 November 2023
Revised 2 February 2024
18 February 2024
Accepted 18 March 2024

Spatiotemporal climate variability and extremes in Middle Awash Afar region Ethiopia: implications to pastoralists and agro-pastoralists food security

Ameha Tadesse Aytenfisu
Center for Food Security Studies, College of Development Studies, Addis Ababa University, Addis Ababa, Ethiopia

Degefa Tolossa
Center for Rural Development Studies, College of Development Studies, Addis Ababa University, Addis Ababa, Ethiopia, and

Solomon Tsehay Feleke and Desalegn Yayeh Ayal
Center for Food Security Studies, College of Development Studies, Addis Ababa University, Addis Ababa, Ethiopia

Abstract

Purpose – This study aims to examine the phenomenon of climate variability and its implications for pastoralists and agro-pastoralists food security in Amibara and Awash Fentale districts of the Afar region, Ethiopia.

Design/methodology/approach – The study relied on meteorological records of temperature and rainfall in the study area between 1988 and 2018. Besides, literature on the topic was reviewed to make caveats on the literal picture that comes from quantitative data, and that is the contribution of this study to the existing debate on climate change and variability. The spatiotemporal trend was determined using the Mann–Kendall test and Sen's slope estimator, while variability was analyzed using the coefficient of variation and standardized anomaly index, and standardized precipitation index/standardized precipitation evapotranspiration index were applied to determine the drought frequency and severity.

Findings – The result reveals that the mean seasonal rainfall varies from 111.34 mm to 518.74 mm. Although the maximum and minimum rainfall occurred in the summer and winter seasons, respectively, there has been a decrease in seasonal and annual at the rate of 2.51 mm per season and 4.12 mm per year, respectively. The study sites have been experiencing highly seasonal rainfall variability. The drought analysis result confirms that a total of nine agricultural droughts ranging from moderate to extreme years were observed. Overall, the seasonal and annual rainfall of the Amibara and Awash Fentale districts showed a decreasing trend with highly temporal variations of rainfall and ever-rising temperatures, and frequent drought events means the climate situation of the area could adversely affect pastoral and agro-pastoral households' food security. However, analysis of data

International Journal of Climate Change Strategies and Management
Vol. 16 No. 2, 2024
pp. 228-252
Emerald Publishing Limited
1756-8692
DOI 10.1108/IJCCSM-11-2023-0140

from secondary sources reveals that analyzing precipitation just based on the meteorological records of the study area would be misleading. That explains why flooding, rather than drought, is becoming the main source of catastrophe to pastoral and agro-pastoral livelihoods.

Practical implications – The analysis of temperature and rainfall dynamics in the Afar region, hence the inception of all development interventions, must take the hydrological impact of the neighboring regions which appears to be useful direction to future researchers.

Originality/value – The research is originally conducted using meteorological and existing literature, and hence, it is original. In this research, we utilized a standardized and appropriate methodology, resulting in insights that augment the existing body of knowledge within the field. These insights serve to advance scholarly discourse on the subject matter.

Keywords Climate variability, Climate change, Afar, Livelihoods, Food security, Drought, Flood

Paper type Research paper

1. Introduction

Climate variability poses significant threats to the achievement of sustainable development goals at both global and national levels. Developing countries, particularly those heavily reliant on nature for their economy and livelihoods, face practical and severe consequences from these phenomena (Filho *et al.*, 2022; Pradhan *et al.*, 2022; Birkmann *et al.*, 2022). Ethiopia experiences rising temperatures, unpredictable rainfall patterns, recurrent droughts, irreversible land degradation, worsening structural poverty and chronic food insecurity (IFPRI and UNDP, 2019). Climate variability and extreme events could disrupt the national economy, exacerbating food insecurity, soil erosion, runoff and water resource depletion, impacting livelihoods (Radović and Iglesias, 2019; Shukla *et al.*, 2019). The northeastern lowlands of Ethiopia confront multiple challenges including climate extremes, invasive alien species and pressure from population-induced rangeland degradation. These factors collectively weaken the ecosystem and biodiversity potential of the area, potentially worsening food insecurity (Birkmann *et al.*, 2022; Ayal *et al.*, 2023; IFPRI and UNDP, 2019; Shiferaw *et al.*, 2021; IPCC, 2014).

The climate variables such as temperature, precipitation and humidity are inherently characterized by spatiotemporal variations (Doshi *et al.*, 2023). These variations and associated impacts on the livelihood and food security of the exposed community could be explained by hydrometeorological spatial (local, regional and global) and temporal (daily, seasonal and annual) events distribution behavior (Niang *et al.*, 2014). Drought is among the most recurring hydrometeorological hazards characterized by extended periods of falling precipitation below average and hence, causes pasture and water scarcity. Drought frequency, duration and intensity could vary significantly across regions and over time. The severity of drought and its effect could be exaggerated by non-climatic factors, e.g. rangeland degradation, demographic and institutional factors (Filho *et al.*, 2021; Filho *et al.*, 2020; Ayal *et al.*, 2019). It seems clear that understanding how these variables change across seasons and years at the microlevel is essential for discerning long-term climate trends for adequate and proper intervention (Birkmann *et al.*, 2022; Filho *et al.*, 2022; Shukla *et al.*, 2019).

Cognizant of this reality, this study examines the spatiotemporal trends, distributional behavior and drought situation using observational data. The temporal aspect of climate variability has been reconstructed at seasonal and annual scales. The spatial aspect of climate variability has been reconstructed based on meteorological data throughout the Amibara and Awash Fentale districts. Drought frequency and magnitude were also examined using established drought indices and investigated the patterns of various climate extremes. In so doing, the article attempts to contribute to a deeper understanding of climate variability in a localized setting and its real impacts and potential implications for ecosystems, societies and economies.

2. Methodology

2.1 Description of the study area

The study area is located in Afar administrative region (Zone 3), latitude between 9°06' and 9°69' N and longitude of 40°10' and 40°46' E (Figure 1), with areas of 1,046.41 km^2 and 2,007.05 km^2, respectively (Adnew *et al.*, 2019). The topography of this area is generally flat, with a maximum altitude of up to 1,342 m above sea level.

The climate of the area is hot and semi-arid. The mean annual temperature is estimated at 26.64°C. The mean annual rainfall is 468.69 mm. Precipitation is generally little, irregular and unpredictable and seems to follow a bimodal pattern in February–April and July–August (Figure 2).

2.2 Statistical variability test

Understanding the spatiotemporal trends and variability of rainfall and temperature is best achieved through the integration of observational data and climate models. Historical climate data, gathered from meteorological stations, satellites and remote sensing, provides valuable insights into past climate patterns. In addition, climate models are used to simulate both past and future climate conditions, enabling scientists to analyze trends and variability within a controlled environment. Various statistical techniques, including time series analysis and spatial interpolation, are commonly used to discern patterns and quantify changes in climate variables.

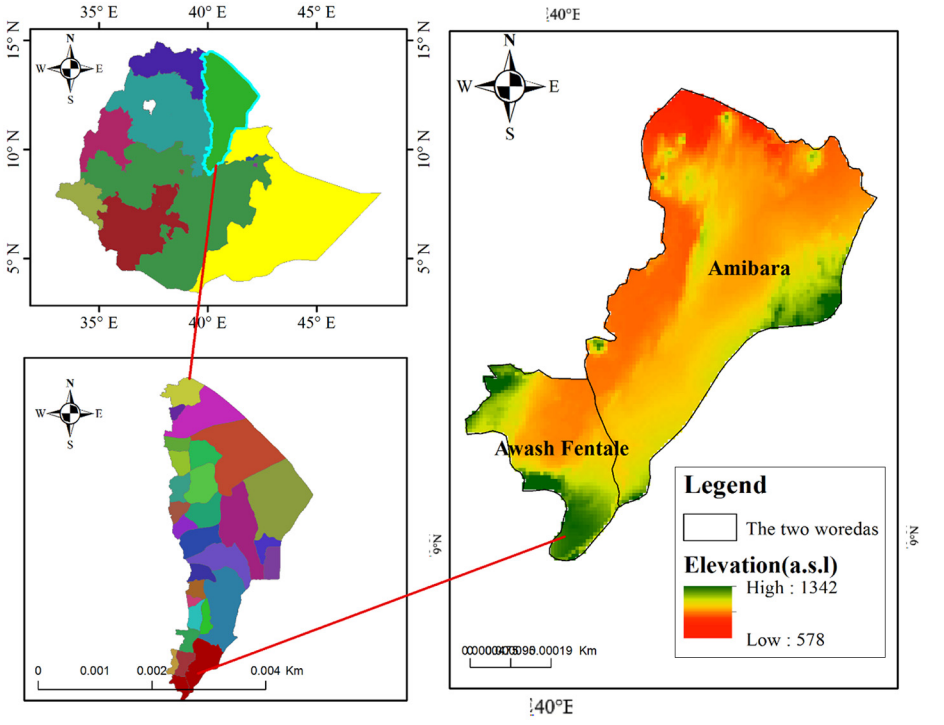

Figure 1.
(a) Location of study area relative to regional divisions of Ethiopia; (b) the whole districts of Afar region and (c) Awash Fentale Woreda and Amibara Woreda Awash in Afar region

Source: Authors' own creation using GIS

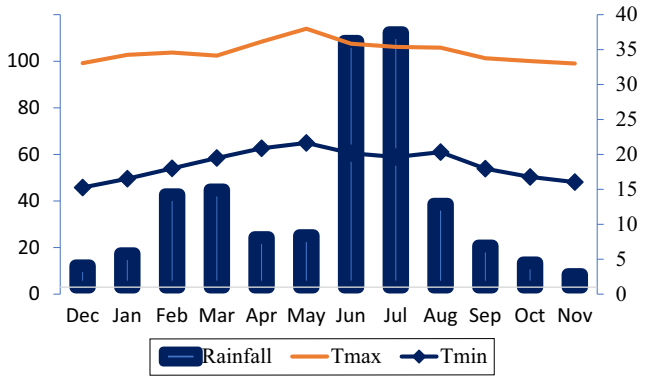

Source: Authors' own creation using National Metrology Institute of Ethiopia Data 2.2

Figure 2. Mean monthly rainfall, mean monthly T-max and mean monthly T-min of the study area

In this study, a range of statistical techniques has been applied to analyze climate data, primarily categorized into variability and trend analysis (Kiros *et al.*, 2016; Koudahe *et al.*, 2017).

Parameters such as mean, standard deviation, median, kurtosis, skewness, range and the coefficient of variance (CV) were used in the analysis process. The CV can be calculated using equation (1):

$$CV = \frac{\sigma}{\mu} \times 100 \qquad 1$$

where σ is the standard deviation, and μ is the mean, CV $<$ 20, less variability; 20 $<$ CV $<$ 30, moderate variability; and CV beyond 30, high variability (Asfaw *et al.*, 2018; Alemayehu *et al.*, 2020)

2.3 Standard anomaly index

Standard anomaly index (SAI) was used to compute negative and positive rainfall and temperature fluctuation anomalies in the study area. The SAI indicates the distance between the data and its mean value (Alemayehu and Bewket, 2017). It is calculated as follows:

$$SAI = \left(\frac{x - \overline{x}}{\sigma}\right) \qquad (1)$$

where x is the rainfall or temperature data, $\overline{x}$ and σ are the mean and the standard deviation of the data, respectively.

2.4 Temporal and spatial trend analysis of climate variables

Different types of tests are available to detect and estimate trends of climate variables. Trend detection can be performed using parametric and nonparametric methods. An example of the parametric method is the linear regression test, and nonparametric (also

called rank-based) methods include the Mann–Kendall test (Mann, 1945; Kendall, 1948). The linear regression model was used to measure the pattern or trend of variables over a long period (Kiros *et al.*, 2016). It is calculated using equation (2).

$$Y = a + bx_t \tag{2}$$

where Y indicates the trend value, a is the intercept, b is the slope of the trend and x_t is the time point.

Mann–Kendall or nonparametric test is applied to analyze the trends of the climate variables. The tests are distribution-free and can tolerate data outliers (Kendall, 1948; Mann, 1945; Yue *et al.*, 2002). The mathematical equations for calculating Mann–Kendall statistics (S) and standardized test statistics Z are as follows (equations (4)–(7)):

$$S = \sum_{i=1}^{N-1} \sum_{j=i+1}^{N} sgn(x_j - x_i) \tag{3}$$

$$sgn(\theta) = \begin{cases} 1 \ if \ (x_j - x_i) > 0 \\ 0 \ if \ (x_j - x_i) = 0 \\ -1 \ if \ (x_j - x_i) < 0 \end{cases} \tag{4}$$

$$V(S) = \frac{1}{18}\left[n(n-1)(2n+5) - \sum_{k=1}^{g} t_k(t_k - 1)(2t_k + 5)\right] \tag{5}$$

$$Z_s = \begin{cases} \dfrac{S-1}{\sqrt{Var(S)}} S > 0 \\ 0, \qquad S = 0 \\ \dfrac{S+1}{\sqrt{Var(S)}} \ S < 0 \end{cases} \tag{6}$$

where N is each number of data points, assuming $(x_j - x_i) = \theta$, the value $sgn(\theta)$ was computed as the signum functioning, which is the number of data points, g is the number of tied groups (a set of data having the same value) and t_k is the number of data series in the k^{th} group. Z is the standard statistics test. The statistical significance level of the trend variation was evaluated using Z_s value. A positive Z_s value indicates an increasing trend, while a negative Z_s value shows a decreasing trend. The null hypothesis *H0* should be rejected if $|Z_s| > Z_{\left(1-\frac{\alpha}{2}\right)}$ *at* the $\alpha = 0.05$ level of significance (Du *et al.*, 2013). However, time-series climate data has positive autocorrelation, increasing the probability of significant output that indirectly leads to a false trend (Alexander *et al.*, 2009; Sa'adi *et al.*, 2019). Thus, this study applied autocorrelation tests of the time series before using the Mann-Kendall (MK) trend test.

2.5 Sen's slope estimator

Sen's slope (Sen, 1968) estimator was used to predict the magnitude of the trend. The nonparametric method can evaluate the change per unit of time. This technique assumes a linear trend in the time series. The slope (Q_i) of all pairs of data x can be calculated as

$$Q_i = \frac{x_{j-X_k}}{j-k}, i = 1, 2, \ldots N, j > k \quad (7)$$

where x_j and x_k are data values of time j and k, respectively. If there are n values in the time series, then there are as many as $n = n(n-1)/2$ slop estimates. The Sen's slope estimator is defined as the median of the n values of Q_i. The values of slopes are ranked from the smallest to the largest, and Sen's slope estimator Q_i is calculated as

If N is an odd observation: $Q_i = Q_{(N+1)/2}$ 8

If N is even observation: $Q_i = \frac{1}{2}\left(Q_{N/2} + Q_{(N+2)/2}\right)$ 9

In this study, each climate variable was analyzed based on four seasons; they were taken as Spring runs from March to May, Summer runs from June to August, Autumn runs from September to October and Winter runs from November to February.

2.6 Test for single change point (Pettiti test)

The Pettitt test has been used in several climate studies to detect abrupt changes in the mean distribution of the variable of interest. It is applied to detect a single change point in climate series with continuous data and gives information about the location of the shift. The test statistic $U_{t,T}$ is evaluated for all random variables from 1 to T; then, the most significant change point is selected where the value of $\lfloor U_{t,T} \rfloor$ is the largest (Jaiswal *et al.*, 2015). To identify a change point, a statistical index U_t is defined as follows:

$$U_{t,T} = \sum_{i=1}^{t} \sum_{j=1}^{T} Sgn(x_i - x_j), \quad 1 \le t \le T \quad (10)$$

where similar to the MK test,

$$Sgn(\theta) = \begin{cases} +1 & \theta > 0 \\ 0 & \theta = 0 \\ -1 & \theta < 0 \end{cases} \quad (11)$$

The most probable change point is found where its value is (the break occurs in year k when). The test statistic Kn and the associated probability (p) used in the test are given as.

$$K_{t_0} = \max_{1 \le y \le n} |U_{t,T}| \quad (12)$$

and the significance probability associated with the value K_t is evaluated as

$$p_{(t_0)} = 2exp\left[\frac{-6k_{t_o}^2}{T^3 + T^2}\right] \quad (13)$$

where t_0 is concluded as a significant change point when $P_{t_0} \le 0.5$. The value is then compared with the critical value (Pettitt, 1979). Given a certain significance level α, if $p < \alpha$, we reject the null hypothesis and conclude that x_t is a significant change point at level α (Du *et al.*, 2013).

2.7 Drought indices

Studying droughts involves assessing their historical occurrence and projected changes in a changing climate. Standardized precipitation index (SPI), the Palmer Drought Severity

Index and the soil moisture anomaly index are widely used to quantify the severity, frequency and spatial extent of drought events at different scales. Moreover, advanced techniques like remote sensing and machine learning are increasingly being used to monitor and predict drought conditions. Different drought indices have been used to analyze drought characteristics in different areas (Morid *et al.*, 2006). This is because a single index does not provide a complete picture of the spatiotemporal distribution of the drought characteristics of the area (Alsafadi *et al.*, 2020; Temam *et al.*, 2019; Tefera *et al.*, 2019; Kourouma *et al.*, 2022). In this study, the two multiscalar (i.e. multiple timescales) drought indices, including the SPI and the SPEI in 3- and 12-month time scales, were used to investigate the occurrence of drought and wet events in the area. The SPI index, the two-parameter Gamma distribution, has been suggested (McKee *et al.*, 1993). The SPEI index is calculated with the three-parameter log-logistic distribution(Vicente-Serrano *et al.*, 2010). Table 1 is used to categorize the dry and wet values of the indices.

2.8 Standardized precipitation index

The SPI evaluates drought in precipitation deficit, impacting groundwater availability, soil moisture streamflow and reservoir storage. Organization (2012) and McKee *et al.* (1993) developed the SPI to analyze precipitation departures from the average precipitation for a particular month or determining time scale. The SPI index is based on the cumulative probability of the considered precipitation. The SPI calculation consists of adjusting the Gamma probability density function to the frequency distribution of the precipitation of each of the rainfall stations. The Gamma probability density function is given by the equation (19).

$$f(x) = \frac{1}{\beta^{\alpha}\Gamma(\alpha)} x^{\alpha-1} e^{-\frac{x}{\beta}} \quad \text{x} > 0 \tag{14}$$

where $\alpha > 0$ is the shape of the parameter, $\beta > 0$ is the scale parameter, $x > 0$ is precipitation and $\Gamma(\alpha)$ is the Gamma function, defined as equation (2).

$$\Gamma(\alpha) = \int_0^{\infty} x^{\alpha-1} e^{-x} dx \tag{15}$$

The parameters α and β of the probability density function are estimated for each station by maximum likelihood (Wilks, 2011).

Table 1. Classification of the severity of dry/wet events on the calculation of SPI/SPEI

Categories	SPI/SPEI values
Extreme drought	Less than −2
Severe drought	−1.99 to −1.50
Moderate drought	−1.49 to −1.00
Near normal	−0.99 to 0.99
Moderately wet	1.00 to 1.49
Severely wet	1.50 to 1.99
Extremely wet	More than 2

Sources: Li *et al.* (2015) and Woldegebrael *et al.* (2020)

$$\hat{\alpha} = \frac{1}{4A}1 + \sqrt{1 + \frac{4A}{3}} \tag{16}$$

$$\hat{\beta} = \frac{\hat{x}}{\hat{\alpha}} \tag{17}$$

$$A = ln\overline{x} - \frac{\sum_i^n x_i}{n} \tag{18}$$

The resulting parameters are then used, and the cumulative probability of the occurrence of a precipitation event for the given month and time scale at the station is considered. The cumulative probability is given by:

$$G(x) = \int_0^x g(x)dx = \frac{1}{\beta^{\gamma}\Gamma(\gamma)_0}\int_0^x x^{\gamma-1}e^{-\frac{x}{\beta}}dx \tag{19}$$

where $\alpha > 0$ is the shape parameter, $\beta > 0$ is the scale parameter, x is the precipitation and $\Gamma(\alpha)$ is the Gamma function, defined as

$$G(x) = \frac{1}{\Gamma(\gamma)}\int_0^x t^{\gamma-1}e^{-t}dt \tag{20}$$

because the gamma function is undefined for $x = 0$ and the precipitation distribution may contain zeros, the cumulative probability becomes:

$$H(x) = q + (1-q)G(x) \tag{21}$$

where q is the probability of zero precipitation. $H(x)$ is then converged into the standard normal SPI variable following approximation (Abramowitz and Stegun, 1965). The normal standardized distribution with null average and the unit variance was then obtained from the transformation of

$$\text{SPI} = \begin{cases} -\left(t - \dfrac{c_0 + c_1 t + c_2 t^2}{1 + d_1 t + d_2 t^2 + d_2 t^3}\right) \; for \; 0 < H(x) \leq 0.5 \\ t = \sqrt{ln\left(\dfrac{1}{H(x)^2}\right)} \\ +\left(t - \dfrac{c_0 + c_1 t + c_2 t^2}{1 + d_1 t + d_2 t^2 + d_2 t^3}\right) \quad for \; 0.5 < H(x) \leq 0.1 \\ t = \sqrt{ln\left(\dfrac{1}{1 - H(x)^2}\right)} \end{cases} \tag{22}$$

$H(x)$ is the cumulative probability of observed precipitation. The coefficient C_0, C_1, C_2 and d_1, d_2, d_3 are given as follows: $C_0 = 2.515517$, $C_1 = 0.802853$, $C_2 = 0.010328$ *and* $d_1 = 1.432788$,

$d_2 = 0.189269$, $d_3 = 0.001308$. The SPI values are symmetrical and can identify both dry and wet conditions. The drought begins when the SPI value becomes negative and ends while returning to a positive value (wet events) (McKee *et al.*, 1993).

2.9 Standardized precipitation evapotranspiration index

The SPEI is multiscalar and used to evaluate different types of global droughts (Labudová *et al.*, 2017; Wang *et al.*, 2014; Yang *et al.*, 2019). The SPEI algorithm is mathematically similar to SPI, but it includes the effect of temperature in addition to precipitation. The SPEI is computed using precipitation (P) and PET as input variables, resulting in the climate water balance (P-PET) outputs (Vicente-Serrano *et al.*, 2010). Including the widely used Penman–Monteith (PM) method, there are several methods have been introduced to calculate (PET) (Allen *et al.*, 1998). However, the PM method requires complete meteorological data, which is challenging in many parts of the world. Thus, the PET can be estimated using the Hargraves (Hargreaves and Samani, 1985) method, which has a similar output as PM (Beguería *et al.*, 2014). Hargraves method needs only precipitation, minimum and maximum temperature and is extraterrestrial radiation (R_a) (Senay *et al.*, 2011). Hence, in this study, the Hargraves method was used to calculate the PET.

$$PET_{HG} = 0.0023 \times (T_{mean} + 17.8) \times \left(\sqrt{T_{max} - T_{min}}\right) \times Ra \tag{23}$$

where PET_{HG} is potential evapotranspiration of the Hargreaves method (mm/day), R_a is the extraterrestrial radiation (mm/day), calculated theoretically as a function of latitude, T-mean is the average temperature (°C) and T-max and T-min are the maximum and minimum temperature (°C), respectively. Once PET was estimated, the water balance equation was used to calculate the monthly deficit (D_i)

$$D_i = P_i - PET_i \tag{24}$$

where D_i is climatic water balance (CWB) in a given period (mm), P_i is monthly precipitation in a given period (mm) and PET_i is the monthly potential evapotranspiration (mm). The accumulated difference between P and PET in different time scales can be calculated as

$$D_n^k == \sum_{i-0}^{k-1} (P_{n-i} - PET_{n-i}) \tag{25}$$

where $n \geq k$, k is a different time scale, and n is the number of calculations.

The function of log-logistic distributions gives better results than other distributions for obtaining SPIE series in standardized D with a mean of zero and standard deviation of one (Potop and Možný, 2011; Vicente-Serrano *et al.*, 2010). The cumulative distribution function $f(x)$ is given by

$$f(x) = \frac{\beta}{\alpha}\left(\frac{x-\gamma}{\alpha}\right)^{\beta-1}\left[1 + \left(\frac{x-\gamma}{\alpha}\right)^{\beta}\right]^{-2} \tag{26}$$

where α, β and γ are scale, shape and location parameters, respectively, for D values in the range ($\gamma < D < \infty$). The probability distribution function of the D series, according to the log-logistic distribution, is given by

$$F(x) = \frac{\beta}{\alpha}\left[1 - \left(\frac{\alpha}{x-\gamma}\right)^{\beta}\right]^{-1} \quad (27)$$

The SPEI can be obtained as the standardized values of $f(x)$.

$$SPEI = W - \frac{C_0 + C_1 W + C_2 W^2}{1 - d_1 W + d_2 W^2 + d_2 W^3} \quad (28)$$

$$W = \sqrt{-2\ln(p)} \text{ for } p \leq 0.5 \quad (29)$$

where p is the probability of exceeding a determined D value, $p = 1 - \mathrm{F}(x)$, if $p > 0.5$, then p is replaced by $1 - p$ and the sign of the resultant SPEI is reversed; the constants are $C_0 = 2.515517$, $C_1 = 0.8022853$, $C_2 = 0.010328$, $d_1 = 1.432788$, $d_2 = 0.189269$ and $d_3 = 0.001308$. Detailed computing of SPEI has been widely described in Vicente-Serrano *et al.* (2010).

SPI/SPEI can be calculated on different time scales, such as 1–3-, 6–12- and 24-months and more (Mathbout *et al.*, 2018). These time scales interpret the different effects of drought on the various types of water resources (McKee *et al.*, 1993; Vilà *et al.*, 2011). This study calculated the SPI and the SPEI indices using a 3–12-month time scale. The three-month time scale is crucial for understanding agricultural drought events, while the 12- and 24-month time scales are exclusively used to analyze hydrological drought events or annual water deficits (Di Giuseppe *et al.*, 2019; Alsafadi *et al.*, 2020; Potop *et al.*, 2012).

2.10 Assessing drought characteristics

Drought characteristics can be expressed by the following essential features: duration, frequency, intensity, severity and spatial and temporal extent (Alamgir *et al.*, 2015; Andreadis *et al.*, 2005). The study evaluated the drought occurrence across months whereby measurements that fall between SPI/SPEI ≤ -1 are further categorized as moderate, severe and extreme drought events. In this research, the assessment of mild drought values was excluded since the variation from the normal level is very slight. The duration, severity, intensity and frequency of the drought events were calculated based on Table 1:

- The frequency is the number of months in which the SPEI value meets a set value (Table 1) divided by the number of months in the entire series (Wang *et al.*, 2014).

$$F = \frac{n}{N} \times 100 \quad (30)$$

where n is the number of months of drought events (SPI/SPEI < -1) that an index value meets a set drought criterion divided by the number of months in the entire series (N). Drought frequency (F) was used to assess the drought prevalence during the study period.

- Duration is monthly or more length drought episodes. Magnitude (M) is the cumulative sum of the index value based on the duration of drought occurrence:

$$M = \sum_{i=1}^{Duration} Index \quad (31)$$

- The intensity of a drought event is the magnitude divided by the duration. Events that have a shorter duration and higher severities will have larger intensities.

$$I = \frac{\text{Magnitude}}{\text{Duration}} \tag{32}$$

The inverse distance weighting method was used to visualize the spatial patterns of climate variability and change.

3. Results and discussion

3.1 Temporal trend of mean seasonal and annual analysis of climate variables

Table 2 depicts the mean seasonal and annual climate variability statistical description and the trend analysis of the study area from 1988 to 2018. The mean seasonal rainfall of the area ranges from 111.34 mm to 518.74 mm. The maximum and minimum rainfall occurred in the summer and winter seasons, respectively. However, in the area a decrease in seasonal and annual rainfall has been decreasing at the rate of 2.51 mm per season and 4.12 mm per year for the past three decades. Relatively, the highest amount of rainfall reduction was observed in the winter season. The rainfall distribution behavior was characterized by high fluctuations all year round. For instance, rainfall distribution was highly variable in spring (CV = 46%), summer (37.95%), autumn (63.75%) and winter (81.96%) (Table 2).

The seasonal and annual maximum and minimum temperatures in the study site vary across seasons. Both seasonal and annual minimum and maximum temperatures increased significantly. The mean seasonal maximum temperature variability ranges from 33.44°C to 34.95°C. The mean seasonal minimum temperature ranges between 18.35°C and 20.48°C. Generally, according to Table 2, the seasonal and annual rainfall of the Amibara and Awash Fentale districts observed a decrease in amount and highly variable in distribution, which means it could affect soil moisture and hence water and pasture availability of the study sites.

Table 2. Statistical summary of seasonal and annual (rainfall, maximum and minimum temperature)

Statistics	Season	Mini	Max	Mean	SD	Kendall's tau	Sen slop	*p*-value	CV*100
Rainfall	Spring	29.42	218.20	111.85	54.58	−0.02	−0.18	0.92	48.00
	Summer	120.90	518.74	246.04	92.39	−0.23	−2.51	0.07	37.9455
	Autumn	19.53	251.08	72.81	46.42	−0.01	−0.12	0.95	63.75
	Winter	3.95	111.34	37.98	30.87	−0.40	−1.61	0.00	81.96
	Annual	220.66	939.61	468.69	133.70	−0.23	−4.12	0.08	28.52
T-max	Spring	27.57	39.99	34.95	2.18	0.24	0.07	0.06	Very high
	Summer	32.89	39.27	36.40	1.47	0.38	0.08	0.00	>>
	Autumn	30.22	36.33	34.13	1.36	0.24	0.05	0.06	>>
	Winter	31.42	36.14	33.44	1.22	0.02	0.00	0.92	>>
	Annual	32.00	37.39	34.73	1.11	0.20	0.03	0.11	>>
T-min	Spring	15.45	23.44	19.46	2.02	0.45	0.15	0.00	>>
	Summer	14.51	24.33	20.48	2.68	0.38	0.15	0.00	>>
	Autumn	13.52	22.28	18.35	2.03	0.43	0.10	0.00	>>
	Winter	12.70	18.29	15.94	1.47	0.18	0.04	0.15	>>
	Annual	15.49	21.50	18.56	1.76	0.38	0.13	0.00	>>
T-mean	Annual	23.78	28.84	26.65	1.22	0.37	0.07	0.00	>>

Source: Authors' own creation using National Metrology Institute of Ethiopia Data

3.2 Standard anomaly index

In this study, analysis of the SAI of hydroclimate data shows the reference line bars above the mean (zero) as positive (surplus), and those below the line mean are negative (deficit) anomalies (Koudahe *et al.*, 2017). The calculated value of SAI obtained was plotted against the year (1988–2018) for annual mean rainfall and maximum and minimum temperatures. Accordingly, in Figure 3, the mean annual rainfall anomaly depicts a negative trend and the coefficient of determination (R^2) of 0.011. Both the mean minimum and maximum temperatures reveal an increasing trend R^2 0.13 and 0.33, respectively. The reinforcing effect of declining rainfall and steadily increasing temperatures could worsen pasture and water availability and, hence, food insecurity in the pastoral areas. It seems clear that the reinforcing effect of decreasing rainfall and increasing temperatures exacerbated the availability and accessibility of pasture and water, leading to heightened food insecurity in the study sites.

3.3 The spatial trend of mean seasonal analysis of climate variables

The Kriging method is widely used for spatial analysis using geographic information systems (GIS). In this study, spatial analysis was applied using the distance-weighting approach through interpolating the data by including information from specific locations. Figure 4 shows a spatial analysis MK trend test using the *Z*-value. Accordingly, in the spring, the rainfall decreased in the northern part of the Amibara district, and an increasing trend was observed in the Awash Fentale district (Figure 4). The spatial analysis result shows that rainfall has been significantly decreasing in the summer season throughout the study sites. However, the summer season rainfall reduction was most pronounced in the southernmost of the Awash Fentale district and northwest of the Amibara district for the past three decades.

Figure 4 shows the study sites have experienced a mix of increasing and decreasing autumn seasonal rainfall. For instance, the southwestern part of the Amibara district received an increase in autumn rainfall while s slight rainfall increment recorded in the southeastern part of the Awash Fentale district. However, it is important to note that except for the southwestern of Amibara and the southeastern part of Awash Fentale the rest parts of the study sites experienced a decrease in rainfall.

The winter season rainfall also observed a significant decreasing rate ($Z < -1.96$) throughout the study sites. In the winter season, the magnitude of the decreasing rainfall is very significant in the southern part of the Awash Fentale district. The spatial seasonal rainfall trend analysis (depicted in Figure 4) reveals that rainfall has been increasing throughout Awash Fentale and the southern part of the Amibara district in the spring season. The northern part of the Amhibara district has been experiencing a remarkable reduction in rainfall in the spring season (see Figure 4).

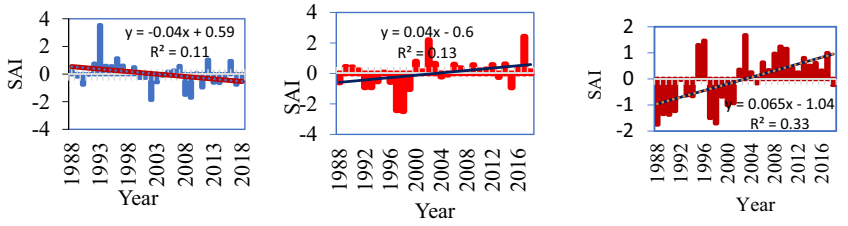

Figure 3. Standard anomaly index of mean annual rainfall and temperature from 1988 to 2018 of the study area

Source: Authors' own creation using National Metrology Institute of Ethiopia Data

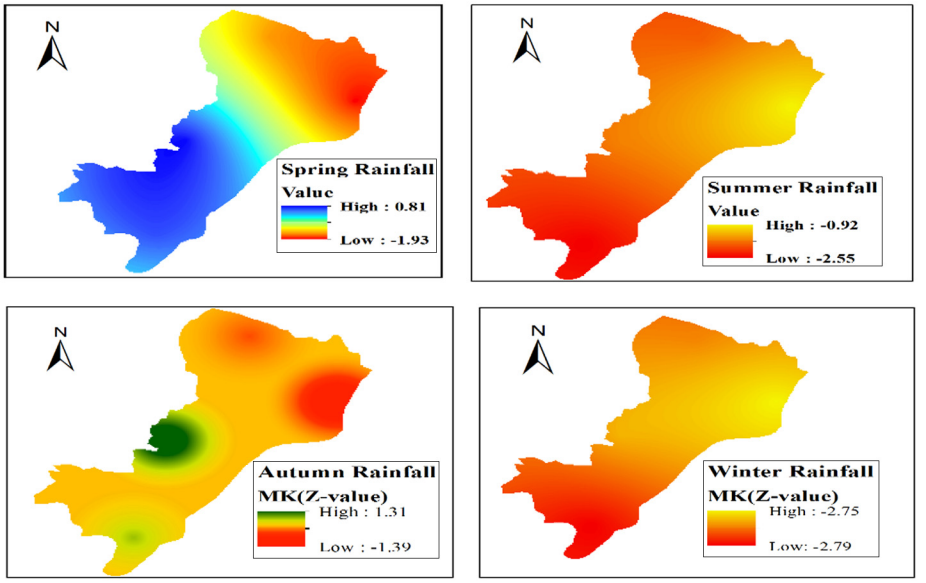

Figure 4.
Spatial trend of seasonal rainfall in the study area from 1988 to 2018

Source: Authors' own creation using National Metrology Institute of Ethiopia Data

Figure 5 shows the spatial trend of seasonal maximum temperature increased for the past three decades except in the southwest and northeastern parts of the Amibara district. In the southwest and northeast parts of Amibara district during the winter season, maximum temperature exhibited reduction. Hence, the lowest and pick spring season maximum temperature increment was observed in the southern part of Awash Fentale and the northern part of Amibara district, respectively. The spatial analysis confirms that during the spring and summer seasons, maximum temperature increased from the south to the northern part of the study sites. Whereas maximum temperature increased from north to south during autumn season. Thus, during the autumn season, a pick maximum temperature was recorded in the southern part of Awash Fentale district. The highest winter season maximum temperature was observed in northern Amibara and the southern part of Awash Fentale districts (Figure 5).

Figure 6 depicts the nature of spatial variations in the seasonal minimum temperature trend of the study area from 1988 to 2018. Seasonal minimum temperature has been increasing in the four seasons at different scales. During the spring season, the pattern of minimum temperature has been increasing from south to north of the two districts. However, unlike the maximum season temperature increment, the autumn season minimum temperature increased from north to south while it lacks a pattern during the summer and winter seasons. The spatial minimum temperate pick of the summer season was observed in the southern part of Awash Fentale and the northeastern part of Amibara district. The slow minimum temperature increment rate of the summer season was exhibited along the northern and southern tips of Awash Fentale and the southern part of Amibara districts temperature lack pattern (Figure 6). On the whole, however, the data leads to the unmistakable conclusion that the entire study area experienced an increasing trend in the minimum temperature across all seasons due to reinforcing

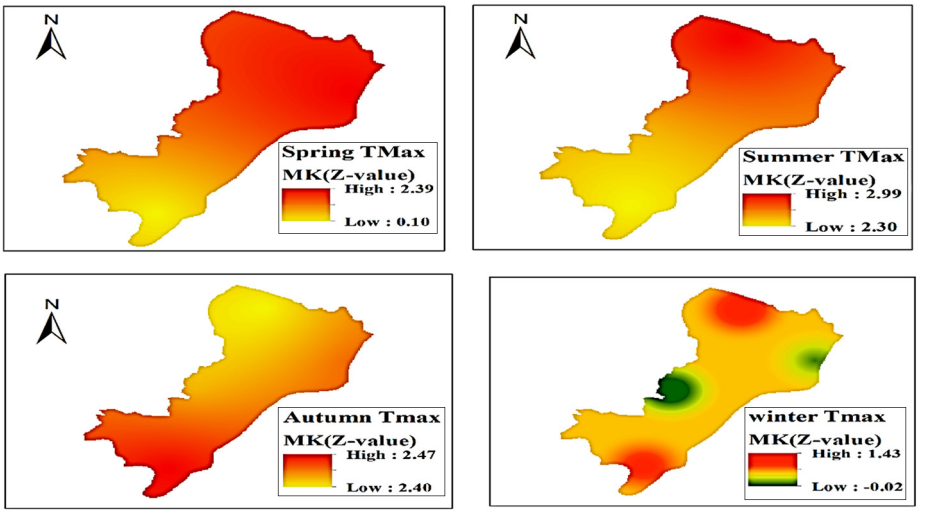

Source: Authors' own creation using National Metrology Institute of Ethiopia Data

Figure 5. Spatial trend of seasonal maximum temperature in the study area from 1988 to 2018

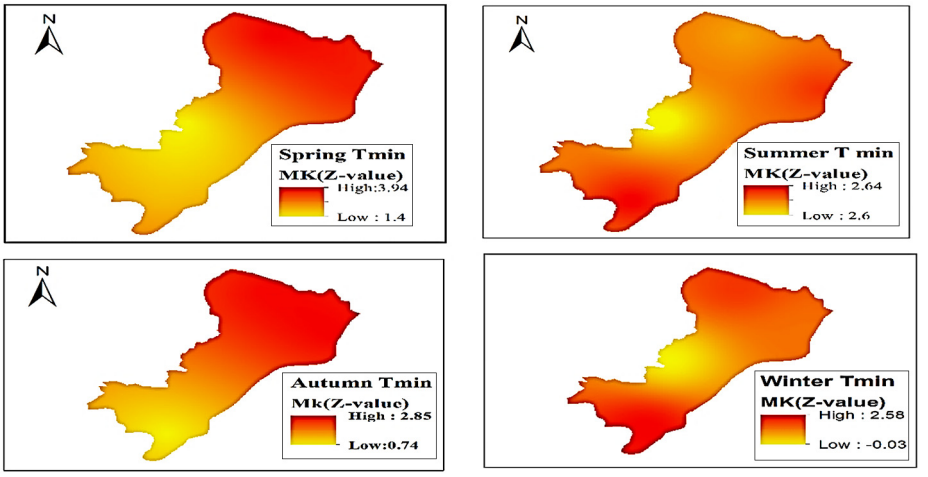

Source: Authors' own creation using National Metrology Institute of Ethiopia Data

Figure 6. Spatial trend of the seasonal minimum temperature of the study area from 1988 to 2018

factors including expansion of agricultural land, settlement and invasive species due to land use land cover change. Thus, the expansion of agricultural land, settlement and invasive species could increase local temperatures and moisture availability by altering land surface characteristics, modifying natural ecosystems and contributing to localized climate changes (Shukla *et al.*, 2019). The cumulative effect of these factors can result in a noticeable effect on pasture and water availability and hence pastoral household food security (Ayal *et al.*, 2023).

3.4 Change points (PETIT) test

Recognizing change points is a statistical technique that plays a vital role in spotting climate jumps in the climatological data period (Palaniswami and Muthiah, 2018). This study used the Pettitt test method to detect the possible change point position and evaluate its statistical significance. The Pettitt test was applied to the annual mean rainfall, minimum temperature and maximum temperature. Accordingly, Figure 7 revealed that the mean annual rainfall experienced a significant decrease in 1999 ($p = 0.037$). The mean annual maximum temperature showed a significant increment in 2001 ($p = 002$). And the mean annual T-min had its significant mean change at the year of 1999 ($p = 0.012$).

3.5 The frequency, distribution and the magnitude of drought events

This study calculated the frequency of the drought events from moderate to extreme drought value based on the threshold value (SPI/SPEI ≤ -1) for the whole study period. From Table 3 below, it is evident that during the study period, the two districts experienced 13% to 37% moderate and above seasonal drought (SPI_3 and SPEI_3-months) frequency. For SPI_12 and SPEI_12 months, the area experienced severe hydrological drought frequency events from 43% to 47%. The peak extreme drought events were observed in all seasons except in the summer season of SPI_3.

3.6 The mean temporal evaluation of drought events

Figure 8 below shows the temporal distribution of drought occurrence over the study area. To evaluate the temporal variation of drought events in the area, those which are consecutively less than a threshold value (SPI/SPEI ≤ -1) and have a duration of more than two months have been selected. Accordingly, in the basin for agricultural drought (SPI_3), categorized from moderate to extreme droughts occurred in 1999, 2000, 2001, 2007, 2008,

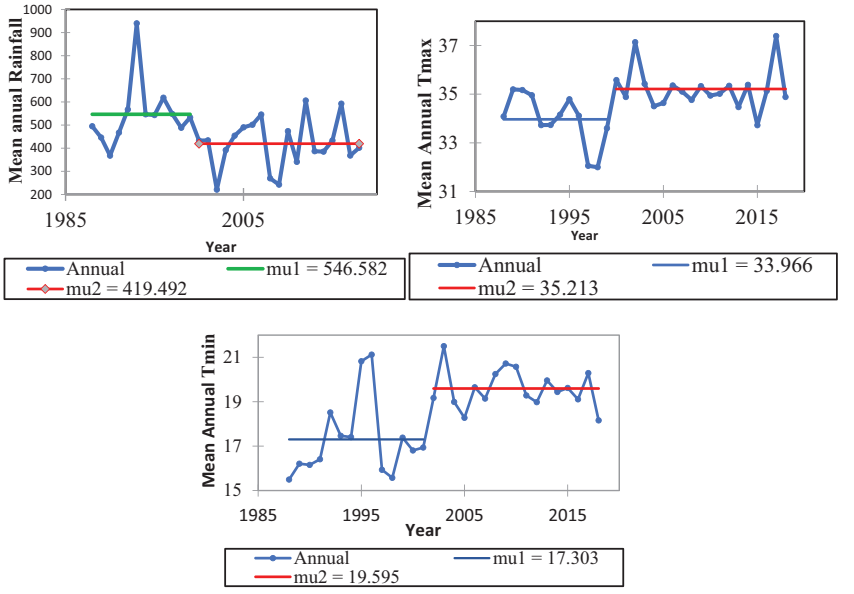

Figure 7.
Changing point and the mean variation for mean annual rainfall, maximum and minimum temperature from 1988 to 2018

Source: Authors' own creation using National Metrology Institute of Ethiopia Data

2011, 2013, 2014 and 2017. For agricultural drought (SPEI_3), moderate to extreme droughts were found in 1999, 2001, 2003, 2007, 2008, 2011, 2012, 2014 and 2017. For hydrological drought (SPI_12), moderate to extreme droughts were found in 1988, 1989, 1999, 2000, 2001, 2002, 2003, 2007, 2008, 2010, 2013, 2016 and 2017. Hydrological drought events (SPEI-12) were identified in 1988, 1989, 1999, 2000, 2001, 2002, 2007, 2008, 2010, 2012, 2013, 2016 and 2017. Generally, in the study period, extreme drought was observed in 1989, 2000, 2001, 2002, 2007, 2010, 2012, 2014 and 2017. In sum, the data analysis on drought events (Figure 8.) revealed the occurrence of seasonal and hydrological drought events at a significant level.

3.7 Implications of climate variability and extremes to food security

From the discussion of the climate data, it has been clearly pointed out that the study area has undergone climate variability, which varied from moderate to extreme levels. That, in turn, reveals that the ecological setting suitable to the age-old agronomic practices has been disrupted. The fluctuation behavior of rainfall and temperature, as well as drought severity would certainly affect the agricultural calendar, soil moisture and pasture availability as well as livestock production and productivity and hence, food security. In sum, the climate variability discerned from metrological data is not something abstract phenomenon but a potent reality that has environmental, socioeconomic, as well as cultural manifestations being observed in the study area. Therefore, it is of a paramount importance to demonstrate the catastrophic impacts of climate variability on people and the physical environment they inhabit.

For a long time, the Afar region rangeland has been characterized by a vegetation cover markedly dominated by different savanna bush, grass and open savannas and woody savannas. Studies reveal that the land use land cover change (LULC) in the Afar region is characterized by 58% Barren land/wasteland (11,501, 000 ha), 3% Grasslands (644, 000 ha), 8% Rainfed-SC-croplands (1,493 000 ha), 6% Irrigated-SC-croplands (1,263 000 ha) and 23% Forest/shrub lands/grasslands (4,531 000 ha) (Gumma *et al.*, 2022). The physical landscape of the Afar region has never been characterized by dense forest cover, even along the Awash River basin. The character of the Afar region rangeland relates to the dominance of open and woody savannah grasslands ideally suitable for grazing and crop cultivation, mainly maize, sorghumand vegetables. That pattern is the norm in the entire lowlands of the Afar region while a few high altitudes exhibit connected woodlands. Therefore, the long-established ecological condition has been exploited by the Afar people both for crop cultivation and animal husbandry (Tessema *et al.*, 2021; Tadese *et al.*, 2019).

Table 3. Drought events frequency, magnitude and peak value in Awash Fentale and Amibara districts (1988 to 2018)

	Tim scale	Duration	Frequency (%)	Magnitude	Peak value
Seasonal drought	Spring	SPI_3	13	−19.5	−4.24
		SPEI_3	23	−34.5	−2.08
	Summer	SPI_3	20	−30	−1.82
		SPEI_3	37	−55.5	−2.11
	Autumn	SPI_3	14	−21	−4.14
		SPEI_3	20	−30	−2.27
	Winter	SPI_3	15	−22.5	−2.83
		SPEI_3	27	−40.5	−2.57
Hydrological drought	Annual drought	SPI_12	43	−64.57%	−3.67
	SPEI_4	SPEI_12	47	−70.5	−2.71

Source: Authors' own creation using National Metrology Institute of Ethiopia Data

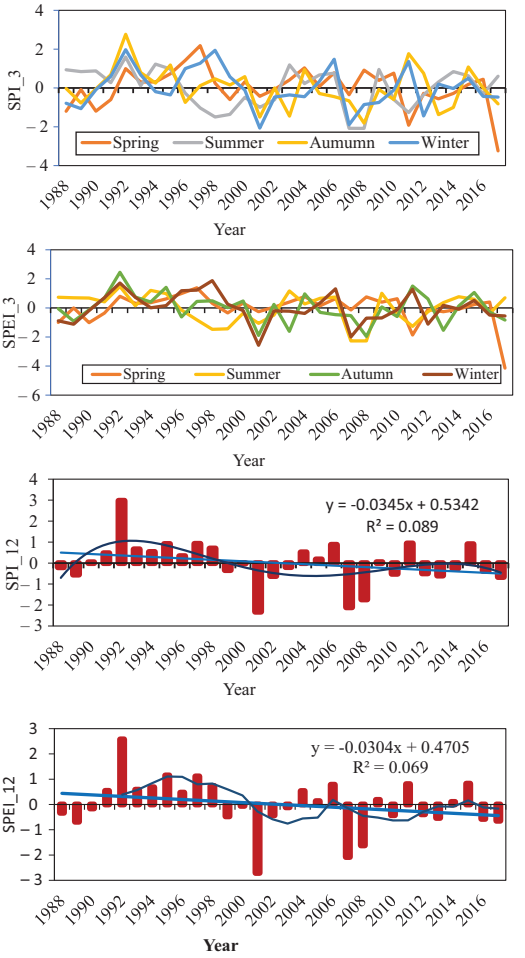

Figure 8.
Trend and variation of different time-scale drought events in the study area for SPI_3. SPEI_3 represents seasonal/agricultural drought, and SPI_12 and SPEI_12 represent annual/hydrological drought in the study period from 1988 to 2018

Source: Authors' own creation using National Metrology Institute of Ethiopia Data

However, in recent decades, the Afar pastoralists and agro-pastoralists are confronted with the phenomenon of vegetation cover dynamics which has a stark correlation with the patterns of climate variability. In the same vein, climate variability characterized by increasing temperature trends has made the occurrence of drought events more frequent and devastating. Not surprisingly, studies in the lowlands of Eritrea, which have a similar ecological setting with the lowlands of the Afar, revealed a similar alarming trend of loss of vegetation cover as analyzed based on seasonal and annual time scales. Analysis of the normalized difference vegetation index showed decreases in the LULC shares of croplands and shrublands. The same study attributed the phenomenon to low moisture caused by drought conditions in the semi-arid region. As is the case elsewhere, the northeast African region is undergoing considerable alteration of vegetation cover and the relative distribution

of different species induced by climate variability that favors the incidence of drought, which disturbs the regeneration and growth pattern of plants (Simon *et al.*, 2019).

The scientific literature concurs on the conventional view that one of the driving factors for the dwindling of natural habitats and biodiversity has to do with the emergence in and colonization of a given environment by invasive plant species. For instance, the glaring disappearance of shrubland biomes is attributable to the invasive plant known as mesquite (Shiferaw *et al.*, 2021). As far as such a phenomenon is the result of natural processes, it has a lot to do with human-induced factors. Strikingly, the occurrence of a devastating invasive plant in the study area and its astonishing expansion is found to be the result of climatological and environmental enabling environment as well as human activities. In this regard, the most peculiar invasive plant prevalent in the study area is known as *Prosopis juliflora*.

To start with, it would be misleading to argue that the origin and expansion of *Prosopis juliflora* in the study area are the result of a spontaneous environmental reaction triggered by the arid environment, decline of rainfall and ever-rising temperatures. Originally, the plant was introduced by human intervention meant to be the best solution to alter bare landmass with lash green vegetation cover in the mid-1970s. The plant was introduced to cover bare lands with green vegetation, to produce firewood, to increase livestock feed and for the purpose of enhancing soil stability (Adnew *et al.*, 2019). In retrospect, however, the measure undertaken without a feasibility study proved to be a catalyst for compounding a preexisting problem of water scarcity. This is because the plant exhausts surface and groundwater throughout the years, especially during the dry season. The unintended effect of introducing *Prosopis juliflora* to the Afar region is that it has posed a formidable threat to the achievement of sustainable development and climate change adaptation (Shiferaw *et al.*, 2021).

Although the appearance of *Prosopis juliflora* in the Afar region has never been a natural response to climate variability, its rapid expansion is attributable to increasing trends in temperature and moisture stress. For a long time, the global concern on the impact of *Prosopis juliflora* has been limited to South America, Central America, South Europe, North Africa and the Caribbean region, dominated by savannahs grasslands (Kyuma *et al.*, 2016). This study found that the environmental setting that allowed the fast spread of *Prosopis juliflora* in those regions exists in the study area and on a more permissive scale. This is because the minimum temperature and frost weather condition that contribute to arresting the expansion of *Prosopis juliflora* in those regions do not exist in the study area. In fact, the typical weather condition in Afar, high temperature and little precipitation, has provided the most suitable ecological conditions for the *Prosopis juliflora* to thrive and expand beyond expectations. The ecological contrast between North African countries and the Afar region explains the sharp contrast in the nature of the problem posed by *Prosopis juliflora*. Whereas *Prosopis juliflora* in North African countries is limited to the original place of plantation (Dakhil *et al.*, 2021), the climatic and environmental factor in the Afar region have offered the plant the right conditions for its unfettered expansion.

The colonization of the Afar region by *Prosopis juliflora* is attributable to the mutually reinforcing factors intrinsic to the nature of the plant itself, as well as the enabling ecological and climatological scenarios. The plant tolerates high temperature. Its deep-reaching roots enable the plant to overcome moisture stress at the expense of underground water. It is naturally endowed with high efficient water use. Its wide canopies prevent other vegetation types from accessing sun light. *Prosopis juliflora* increases soil fertility by augmenting fine soil particles useful for its expansion. The allelochemicals produced by the plant undermine the survival of other species by diminishing their seed germination as well as growth.

Because of such character traits, the traditional vegetation composition of the Afar region has become an easy prey to the predatory invasive plant known as *Prosopis juliflora* (Dakhil *et al.*, 2021; Kyuma *et al.*, 2016).

The rapid expansion of *Prosopis juliflora* in the Afar region is assisted by domestic animals. When domestic animals consume the fruit of *Prosopis juliflora*, the seeds carried in the droppings of animals will be dispersed to long distances, and everywhere they are dropped, the plant grows. Moreover, the nature of climate variability characterized by seasonal and annual temperature increases coupled with the alkaline nature of the soil in the study area has created the right condition for the unmitigated expansion of *Prosopis juliflora*. Hence, the region is confronted with the rapid shrinking of savannah grasslands and bush forests that for long constituted the right ecological condition on which the erstwhile pastoralist livelihood of the Afar people depended (Dakhil *et al.*, 2021). Therefore, the findings of the study neatly tally with a previous finding in Kenya, which argues that a climate variability characterized by erratic and dwindling rainfall coupled with increases in the annual mean temperature nurtures the expansion of *Prosopis juliflora* thereby exacting the feed resource available to the livestock population (Kyuma *et al.*, 2016).

There is an emerging discussion about policy response toward *Prosopis juliflora*. As part of that effort, the pros and cons of the plant are being sorted out. On the positive side, the plant is a good source of food for humans and animals especially during periods of food and feed stress. It is a good source of firewood, biofuel energy, charcoal and timber production (Adnew *et al.*, 2019; Abeje *et al.*, 2019; USAID, 2018). Reports show that local people use the plant to construct their houses and sheds. The plant is also positively evaluated for its benefit regarding flood protection, carbon sequestration, windbreak, treatment for soil salinity and landscape greening. To the contrary, the plant has damaging aspects: undermining the ecosystem services, fostering food insecurity by reducing the volume of milk and meat production. The more *Prosopis juliflora* depletes animal pasture, animals lose body weight and their market price gets smaller *(*Adnew *et al.*, 2019*)*. Livestock health is being affected by the plant, which causes a disease local people, "Armko," which arises when animals consume the raw seeds of *Prosopis*. On balance, the adverse effects of *Prosopis juliflora* on ecological resources, socioeconomic conditions, development projects, urban areas and national parks outweigh its controversial benefits (Adnew *et al.*, 2019).

Apparently, there seems to be a contradictory argument in the literature about the chronic shortage of precipitation on the one hand and the recurrent problem of flooding. As discussed above, the analysis of climatic data in this study spanning 30 years offers a compelling argument for climate variability characterized by increment of temperature and decrement of precipitation. Our argument is that the temperature and rainfall measurements in metrological stations offer a misleading impression about the water resources available in the Afar region. For a balanced assessment of water resources available to the Afar region, one must look at the fact that the lowlands of Afar are natural absorbents of heavy rainfall water from the Amhara, Tigrai and central Ethiopia (USAID, 2018). As a result, the Afar region is naturally bound to be a victim or beneficiary of climate phenomena in the Ethiopian highlands. For instance, the massive flooding that occurred in 2010 had damaged considerable crops, infrastructure, irrigation systems and livestock. In the Afar region, about 67,000 people were affected by the flood (HOUSE, 2011). Similarly, a flood incident in 2020 impacted 67,885 individuals, displacing 40,731 people and putting 32,839 people at risk. Further, the adverse impact of the flood incident involved the evacuation of 4,915 people, the destruction of 100 education and health centers and the loss of 16,626 livestock (OCHA, 2020). Table 4 suggests that in the Afar region, recurrent flooding rather than drought is the primary factor responsible for crop damage compared to other regional states.

Region	Dominant hazard in cropland damage	Seasonal dynamic of hazard	Dominant hazard contributing to loss of cattle
Amhara	Hail 100%	August–September corresponding to the Kiremt season	Hailstorms
Oromia	Fire 82% Floods 14%	Fires: September flood: March and September	Drought
SNNPR	Drought 13% Flood 12%	Floods: September to December	Flood
Afar	Drought 13% Floods 47%	Drought: March and September Floods: July to November	Floods
Tigray	Drought 58% Floods 35% Hailstorm 8%	Drought: September Floods: June to December Hailstorm: July to December	Hailstorm

Source: USAID (2018)

Table 4.
Crop damage by geographic area and source

Finally, the impact of climate variability and the expansion of *Prosopis juliflora* need to be discussed in light of the strong drive of the government to make the Afar region a vital target of food security through wheat production. In view of the growing demand for wheat, the policy direction of the government to substitute wheat import through local production, the government has made the Afar region one of the priority areas for irrigation-based wheat production. The government is trying to cover 1.5 million hectares in the coming five years with wheat production (Tadesse *et al.*, 2022). In view of the clear danger posed on this ambitious project by the *Prosopis juliflora* invasive plant, the need to overcome the threat of climate variability on food security requires an all-inclusive approach.

4. Conclusions and recommendations

The study has established the characteristics, manifestations, trends and magnitude of climate variability as witnessed in the Awash Fentale and Amibara districts of the Afar National Regional State. The two main sources of data were measurements of temperature and precipitation taken *in situ* that span 30 years of temporal horizon. For analysis of the impact of climate variability, the study investigated contemporary reports of pertinent organizations and published articles. Based on analysis of statistical results and periodic reports, it is concluded that the study areas have witnessed extreme climate variability where the main pattern is neither substantial nor directional increases or decreases in measurements of temperature and rainfall. Rather, the peculiar feature of climate variability in the two districts is erratic and highly unpredictable temperature and precipitation. The erratic and unpredictable characteristics of climate variability have been further compounded by the indelible impact of weather conditions in northern and central Ethiopia on the lowlands of the Afar region. Since the Afar region is geographically situated to be on the receiving end of excess precipitation in central and northern Ethiopian highlands, analysis of precipitation merely based on meteorological records is proved to be superficial.

From the above conclusion, it is recommended that policy design and implementation about the management of climate variability while ensuring food security best suited to the Afar natural ecological landscape and the traditional livelihood practices must take elements and conditions of the weather phenomenon on the entire north Ethiopian region. Because the Afar region gets more precipitation from the flow of floods in central and north

Ethiopia, agronomic technologies fare better from the application of floodwater technologies rather than the propagation of rainfall-based agricultural technologies. Therefore, the ongoing policy drive for irrigation-based wheat production is highly commended by the findings of this research. Finally, it should be pointed out that the prospect of harnessing climate change-friendly livelihoods for an ideal level of food security requires the concerted and coordinated efforts of all stakeholders toward the eventual elimination of the invasive plant called *Prosopis juliflora*.

References

Abeje, M.T., Tsunekawa, A., Haregeweyn, N., Nigussie, Z., Adgo, E., Ayalew, Z., Tsubo, M., Elias, A., Berihun, D. and Quandt, A. (2019), "Communities' livelihood vulnerability to climate variability in Ethiopia", *Sustainability*, Vol. 11 No. 22, pp. 6302-6322.

Abramowitz, M. and Stegun, I.A. (1965), "With formulas, graphs, and mathematical tables *N*ational Bureau of *S*tandards Applied Mathematics series", *e*, Vol. 55, p. 953.

Adnew, M., Assen, M. and Tesfay, M. (2019), *Prosopis Juliflora: Impacts and Management in the Face of Climate Change in Ethiopia's Middle Awash Valley ASSAR*, University of Cape Town.

Alamgir, M., Shahid, S., Hazarika, M.K., Nashrrullah, S., Harun, S.B. and Shamsudin, S. (2015), "Analysis of meteorological drought pattern during different climatic and cropping seasons in Bangladesh", *JAWRA Journal of the American Water Resources Association*, Vol. 51 No. 3, pp. 794-806.

Alemayehu, A. and Bewket, W. (2017), "Local spatiotemporal variability and trends in rainfall and temperature in the Central Highlands of Ethiopia", *Geografiska Annaler: Series A, Physical Geography*, Vol. 99 No. 2, pp. 85-101.

Alemayehu, A., Maru, M., Bewket, W. and Assen, M. (2020), "Spatiotemporal variability and trends in rainfall and temperature in alwero watershed, Western Ethiopia", *Environmental Systems Research*, Vol. 9pp No. 1, p. 15.

Alexander, L.V., Tapper, N., Zhang, X., Fowler, H.J., Tebaldi, C. and Lynch, A. (2009), "Climate extremes: progress and future directions", *International Journal of Climatology*, Vol. 29 No. 3, pp. 317-319.

Allen, R.G., Pereira, L.S., Raes, D. and Smith, M. (1998), "Crop evapotranspiration-guidelines for computing crop water requirements FAO irrigation and drainage paper 56", *Fao, Rome*, Vol. 300, p. D05109.

Alsafadi, K., Mohammed, S., Ayugi, B., Sharaf, M. and Harsányi, E. (2020), "Spatial–temporal evolution of drought characteristics over Hungary between 1961 and 2010", *Pure and Applied Geophysics*, Vol. 177 No. 8, pp. 3961-3978.

Andreadis, K.M., Clark, E.A., Wood, A.W., Hamlet, A.F. and Lettenmaier, D.P. (2005), "Twentieth-century drought in the conterminous United States", *Journal of Hydrometeorology*, Vol. 6 No. 6, pp. 985-1001.

Asfaw, A., Simane, B., Hassen, A. and Bantider, A. (2018), "Variability and time series trend analysis of rainfall and temperature in northcentral Ethiopia: a case study in Woleka Sub-basin", *Weather and Climate Extremes*, Vol. 19, pp. 29-41.

Ayal, D.Y., Desta, S. and Robinson, L. (2019), "Governance dimensions of climate change adaptation: the case of Didahara, Borana, Southern Ethiopia", in Leal Filho W. (Eds), *Handbook of Climate Change Resilience*, Springer, Cham, doi: 10.1007/978-3-319-71025-9_172-1.

Ayal, D.Y., Nure, A., Tesfaye, B., Ture, K. and Zeleke, T.T. (2023), "An appraisal on the determinants of adaptation responses to the impacts of climate variability on coffee production: Implication to household food security in Nensebo Woreda, Ethiopia", *Climate Services*, Vol. 30, p. 100383.

Beguería, S., Vicente-Serrano, S.M., Reig, F. and Latorre, B. (2014), "Standardized precipitation evapotranspiration index (SPEI) revisited: parameter fitting, evapotranspiration models, tools,

datasets and drought monitoring", *International Journal of Climatology*, Vol. 34 No. 10, pp. 3001-3023.

Birkmann, J., Jamshed, A., Mcmillan, J.M., Feldmeyer, D., Totin, E., Solecki, W., Ibrahim, Z.Z., Roberts, D., Kerr, R.B. and Poertner, H.O. (2022), "Understanding human vulnerability to climate change: a global perspective on index validation for adaptation planning", *Science of the Total Environment*, Vol. 803, p. 150065.

Dakhil, M.A., El-Keblawy, A., El-Sheikh, M.A., Halmy, M.W.A., Ksiksi, T. and Hassan, W.A. (2021), "Global invasion risk assessment of *Prosopis Juliflora* at biome level: does soil matter?", *Biology*, Vol. 10 No. 3, p. 89.

Di Giuseppe, E., Pasqui, M., Magno, R. and Quaresima, S. (2019), "A counting process approach for trend assessment of drought condition", *Hydrology*, Vol. 6 No. 4, pp. 28-82.

Doshi, S.C., Lohmann, G., Rimbu, N. and Ionita, M. (2023), "Spatiotemporal trend analysis of climate indices for the European continent", *Journal of Water and Climate Change*, Vol. 14 No. 9, pp. 3112-3130.

Du, J., Fang, J., Xu, W. and Shi, P. (2013), "Analysis of dry/wet conditions using the standardized precipitation index and its potential usefulness for drought/flood monitoring in Hunan province, China", *Stochastic Environmental Research and Risk Assessment*, Vol. 27 No. 2, pp. 377-387.

Filho, W.L., Azeiteiro, U.M.A.-L., Balogun, A.F.F., Setti, S.A.R., Mucova, Ayal, D.Y., E., Totin, A., M.L., Felix, K.K. and Nicholas, O.O. (2021), "The influence of ecosystems services depletion to climate change adaptation efforts in Africa", *Science of the Total Environment*, Vol. 779, p. 146414, doi: 10.1016/j.scitotenv.2021.146414.

Filho, W.L., Stojanov, R., Wolf, F., Matandirotya, N.R., Ploberger, C., Ayal, D.Y., Azam, F.M.S., Al-Ahdal, T.M.A., Sarku, R. and Tchouaffe Tchiadje, N.F. (2022), "Assessing uncertainties in climate change adaptation and land management", *Land*, Vol. 11 No. 12, p. 2226, doi: 10.3390/land11122226.

Filho, W., Taddese, H., Balehegn, M., Nzengya, D., Debela, N., Abayineh, A., Mworozi, E., Osei, S., Ayal, D., Nagy, G., Yannick, N., Kimu, S., Balogun, A.-L., Alemu, E., Li, C., Sidsaph, H. and Wolf, F. (2020), "Introducing experiences from African pastoralist communities to cope with climate change risks, hazards and extremes: fostering poverty reduction", *International Journal of Disaster Risk Reduction*, Vol. 50 No. 101738, pp. 1-11.

Gumma, M.K., Amede, T., Getnet, M., Pinjarla, B., Panjala, P., Legesse, G., Tilahun, G., Van Den Akker, E., Berdel, W. and Keller, C. (2022), "Assessing potential locations for flood-based farming using satellite imagery: a case study of Afar region, Ethiopia", *Renewable Agriculture and Food Systems*, Vol. 37 No. S1, pp. S28-S42, doi: 10.1017/S1742170519000516.

Hargreaves, G.H. and Samani, Z.A. (1985), "Reference crop evapotranspiration from temperature", *Applied Engineering in Agriculture*, Vol. 1, pp. 96-99.

House, A.P.C. (2011), *Livelihoods-Based Flood Emergency Response Project in Afar Regional State External Evaluation Report ABCON Plc*, Consulting House, Addis Ababa, Ethiopia.

IFPRI and UNDP (2019), "*International Food Policy Research Institute. Building Resilience To Climate Shocks In Ethiopia*", Washington, DC, doi: 10.2499/9780896293595.

IPCC (2014), *Climate Change: Synthesis Report. Contribution of Working Groups I, II and III to the Fifth Assessment Report of Intergovernmental Panel on Climate Change* Core Writing Team, Pachauri, R.K. and Meyer, L.A. (Eds), IPCC, Geneva, Switzerland, p. 151.

Jaiswal, R., Lohani, A. and Tiwari, H. (2015), "Statistical analysis for change detection and trend assessment in climatological parameters", *Environmental Processes*, Vol. 2 No. 4, pp. 729-749.

Kendall, M.G. (1948), *Rank Correlation Methods*, Charles Griffin, London.

Kiros, G., Shetty, A. and Nandagiri, L. (2016), "Analysis of variability and trends in rainfall over Northern Ethiopia", *Arabian Journal of Geosciences*, Vol. 9 No. 6, pp. 1-12.

Koudahe, K., Kayode, A.J., Samson, A.O., Adebola, A.A. and Djaman, K. (2017), "Trend analysis in standardized precipitation index and standardized anomaly index in the context of climate change in Southern Togo", *Atmospheric and Climate Sciences*, Vol. 7 No. 4, pp. 401-423.

Kourouma, J.M., Eze, E., Kelem, G., Negash, E., Phiri, D., Vinya, R., Girma, A. and Zenebe, A. (2022), "Spatiotemporal climate variability and meteorological drought characterization in Ethiopia", *Geomatics, Natural Hazards and Risk*, Vol. 13 No. 1, pp. 2049-2085.

Kyuma, R., Wahome, R., Kinama, J. and Wasonga, V. (2016), "Temporal relationship between climate variability, *Prosopis Juliflora* invasion and livestock numbers in the drylands of MAGADI, Kenya", *African Journal of Environmental Science and Technology*, Vol. 10 No. 4, pp. 129-140.

Labudová, L., Labuda, M. and Takáč, J. (2017), "Comparison of SPI and SPEI applicability for drought impact assessment on crop production in the Danubian lowland and the east Slovakian lowland", *Theoretical and Applied Climatology*, Vol. 128 Nos 1/2, pp. 491-506.

Li, X., He, B., Quan, X., Liao, Z. and Bai, X. (2015), "Use of the standardized precipitation evapotranspiration index (SPEI) to characterize the drying trend in southwest China from 1982–2012", *Remote Sensing*, Vol. 7 No. 8, pp. 10917-10937.

Mckee, T.B., Doesken, N.J. and Kleist, J. (1993), "The relationship of drought frequency and duration to time scales", *Proceedings of The 8th Conference On Applied Climatology, 1993. CA*, pp. 179-183.

Mann, H.B. (1945), "Nonparametric tests against trend", *Econometrica*, Vol. 13 No. 3, pp. 245-259.

Mathbout, S., Lopez-Bustins, J.A., Martin-Vide, J., Bech, J. and Rodrigo, F.S. (2018), "Spatial and temporal analysis of drought variability at several time scales in Syria during 1961–2012", *Atmospheric Research*, Vol. 200, pp. 153-168.

Morid, S., Smakhtin, V. and Moghaddasi, M. (2006), "Comparison of seven meteorological indices for drought monitoring in Iran", *International Journal of Climatology*, Vol. 26 No. 7, pp. 971-985.

Niang, I., Ruppel, O.C., Abdrabo, M.A., Essel, A., Lennard, C., Padgham, J., Urquhart, P. (2014), "Africa—Chapter 22", in Barros, V.R., Field, C.B., Dokken, D.J., Mastrandrea, M.D., Mach, K.J., Bilir, T.E., Chatterjee, M., Ebi, K.L., Estrada, Y.O., Genova, R.C., Girma, B., Kissel, E.S., Levy, A.N., MacCracken S., Mastrandrea, P.R. and White, L.L. (Eds), *Climate Change 2014: Impacts, Adaptation, and Vulnerability Part b: Regional Aspects. Contribution of Working Group II.; Fifth Assessment Report of the Intergovernmental Panel on Climate Change*, Cambridge University Press, Cambridge, pp. 1199-1265.

Ocha (2020), *Afar Region: Flood Snapshot*, Ethiopia.

Organization, W.M. (2012), *Standardized Precipitation Index User Guide*, World Meteorological Organization, p. 1090.

Palaniswami, S. and Muthiah, K. (2018), "Change point detection and trend analysis of rainfall and temperature series over the Vellar river basin", *Polish Journal of Environmental Studies*, Vol. 27 No. 4, pp. 673-1681.

Pettitt, A.N. (1979), "A non-parametric approach to the change-point problem", *Journal of the Royal Statistical Society*, Vol. 28 No. 2, pp. 126-135.

Potop, V. and Možný, M. (2011), "Examination of the effect of evapotranspiration as an output parameter in SPEI drought index in Central Bohemian region", in Šiška, B., Hauptvogl, M. and Eliašová, M. (Eds), Bioclimate: Source and Limit of Social Development, International Scientific Conference, 6th–9th September 2011, Topoľčianky, Slovakia.

Potop, V., Možný, M. and Soukup, J. (2012), "Drought evolution at various time scales in the lowland regions and their impact on vegetable crops in the Czech Republic", *Agricultural and Forest Meteorology*, Vol. 156, pp. 121-133.

Pradhan, P., Seydewitz, T., Zhou, B., Lüdeke, M.K., Kropp, J.P. (2022), "Climate extremes are becoming more frequent, co-occurring, and persistent in Europe", *Anthropocene Science*, Vol. 1 No. 2, pp. 264-277.

Radović, V. and Iglesias, I. (2019), "Extreme weather events: Definition, classification, and guidelines towards vulnerability reduction and adaptation management", Climate Action, Springer.

Sa'adi, Z., Shahid, S., Ismail, T., Chung, E.-S. and Wang, X.-J. (2019), "Trends analysis of rainfall and rainfall extremes in Sarawak, Malaysia using modified Mann–Kendall test", *Meteorology and Atmospheric Physics*, Vol. 131 No. 3, pp. 263-277.

Sen, P.K. (1968), "Estimates of the regression coefficient based on Kendall's tau", *Journal of the American Statistical Association*, Vol. 63 No. 324, pp. 1379-1389.

Senay, G., Leake, S., Nagler, P., Artan, G., Dickinson, J., Cordova, J. and Glenn, E. (2011), "Estimating basin scale evapotranspiration (ET) by water balance and remote sensing methods", *Hydrological Processes*, Vol. 25 No. 26, pp. 4037-4049.

Shiferaw, H., Alamirew, T., Dzikiti, S., Bewket, W., Zeleke, G. and Schaffner, U. (2021), "Water use of *Prosopis Juliflora* and its impacts on catchment water budget and rural livelihoods in Afar region, Ethiopia", *Scientific Reports*, Vol. 11 No. 1, p. 2688, doi: 10.1038/s41598-021-81776-6.

Shukla, P.R., Skeg, J., Buendia, E.C., Masson-Delmotte, V., Pörtner, H.O., Roberts, D.C., Zhai, P., Slade, R., Connors, S., Van Diemen, S. and Ferrat, M. (2019), "Climate change and land: an IPCC special report on climate change, desertification, land degradation, sustainable landmanagement, food security, and greenhouse gas fluxes in terrestrial ecosystems".

Simon, A., Katzensteiner, K. and Gratzer, G. (2019), "Drivers of forest regeneration patterns in drought prone mixed-species forests in the Northern Calcareous Alps", *Forest Ecology and Management*, Vol. 453, p. 117589, doi: 10.1016/j.foreco.2019.117589.

Tadese, M.T., Kumar, L., Koech, R. and Zemadim, B. (2019), "Hydro-climatic variability: a characterisation and trend study of the Awash River Basin, Ethiopia", *Hydrology*, Vol. 6 No. 2, pp. 35-29.

Tadesse, W., Zegeye, H., Debele, T., Kassa, D., Shiferaw, W., Solomon, T., Negash, T., Geleta, N., Bishaw, Z. and Assefa, S. (2022), "Wheat production and breeding in Ethiopia: retrospect and prospects", *Crop Breeding, Genetics and Genomics*, Vol. 4 No. 3 e220003, p. 1.

Tefera, A.S., Ayoade, J. and Bello, N. (2019), "Drought occurrence pattern in Tigray region, Northern Ethiopia", *Journal of Applied Sciences and Environmental Management*, Vol. 23 No. 7, pp. 1341-1348.

Temam, D., Uddameri, V., Mohammadi, G., Hernandez, E.A. and Ekwaro-Osire, S. (2019), "Long-term drought trends in Ethiopia with implications for dryland agriculture", *Water*, Vol. 11 No. 12, p. 2571.

Tessema, N., Kebede, A. and Yadeta, D. (2021), "Modelling the effects of climate change on streamflow using climate and hydrological models: the case of the Kesem Sub-basin of the Awash River Basin, Ethiopia", *International Journal of River Basin Management*, Vol. 19 No. 4, pp. 469-480.

USAID (2018), "Climate variability and change in Ethiopia summary of findings. Ethiopia".

Vicente-Serrano, S.M., Beguería, S. and López-Moreno, J.I. (2010), "A multiscalar drought index sensitive to global warming: the standardized precipitation evapotranspiration index", *Journal of Climate*, Vol. 23 No. 7, pp. 1696-1718.

Vilà, M., Espinar, J.L., Hejda, M., Hulme, P.E., Jarošík, V., Maron, J.L., Pergl, J., Schaffner, U., Sun, Y. and Pyšek, P. (2011), "Ecological impacts of invasive alien plants: a meta-analysis of their effects on species, communities and ecosystems", *Ecology Letters*, Vol. 14 No. 7, pp. 702-708.

Wang, Q., Wu, J., Lei, T., He, B., Wu, Z., Liu, M., Mo, X., Geng, G., Li, X. and Zhou, H. (2014), "Temporal-spatial characteristics of severe drought events and their impact on agriculture on a global scale", *Quaternary International*, Vol. 349, pp. 10-21.

Wilks, D.S. (2011), *Statistical methods in the atmospheric sciences*, Academic Press.

Woldegebrael, S.M., Berhanu, B., Zaitchik, B. and Melesse, A.M. (2020), "Rainfall and flood event interrelationship—a case study of awash and Omo-Gibe basins, Ethiopia", *International Journal of Scientific and Engineering Research*, Vol. 11 No. 1, pp. 332-343.

Yang, C., Tuo, Y., Ma, J. and Zhang, D. (2019), "Spatial and temporal evolution characteristics of drought in Yunnan province from 1969 to 2018 based on SPI/SPEI", *Water, Air, and Soil Pollution*, Vol. 230 No. 11, pp. 1-13.

Yue, S., Pilon, P. and Cavadias, G. (2002), "Power of the Mann–Kendall and Spearman's rho tests for detecting monotonic trends in hydrological series", *Journal of Hydrology*, Vol. 259 Nos 1/4, pp. 254-271.

Corresponding author
Desalegn Yayeh Ayal can be contacted at: desalula@gmail.com